Hindawi
Scientific Programming
Volume 2022, Article ID 5984948, 12 pages
https://doi.org/10.1155/2022/5984948

Research Article

The Design of Urban Sculpture Space with User Behavior Based on Internet of Things and Edge Computing

Chili He

School of Architecture, South China University of Technology, Guangzhou 510641, China

Correspondence should be addressed to Chili He; arhcl@scut.edu.cn

Received 15 March 2022; Revised 18 May 2022; Accepted 31 May 2022; Published 8 July 2022

Academic Editor: Y. P. Tsang

To solve the application of Virtual Reality (VR) technology in the design of urban sculpture space, a VR network model is implemented based on Internet of Things (IoT) and Edge Computing. First, this work expounds and analyzes the theory of urban sculpture space and the interaction of urban sculpture space. Second, aiming at the problem that the development of IoT cannot meet the large amount of data and low delay of VR, a resource allocation algorithm, Joint Optimization of Resource Allocation and FOV (J-RAF) strategy is proposed based on the user interest and the resource allocation problem of (FOV), and simulation experiments are used to verify the effectiveness of the J-RAF algorithm. Finally, a VR network system is established based on cache cooperation and user interest, and a resource allocation algorithm Joint Cooperative Content Caching and FOV (J-CCF) is proposed, and its effectiveness is verified. Experiments show that compared with random strategy and random viewport strategy, algorithm J-CCF has 3% and 20% system gain. Compared with noncooperative cache scheme and random viewport strategy, algorithm J-CCF can improve the system gain by 15% and 25%, respectively. It is verified that the convergence of J-RAF algorithm and J-CCF algorithm and the effectiveness of improving the system gain. This work provides a technical basis for optimizing the design method of urban sculpture and contributes to the optimal design of urban space.

1. Introduction

With the development of the Internet of Things (IoT), a variety of new technologies emerge in endlessly. The traditional urban sculpture can no longer meet people's functional needs for urban sculpture space [1]. The combination of IoT technology and urban sculpture space has greatly improved the interactivity compared with traditional urban sculpture [2]. Urban sculpture, using IoT technology pays more attention to users' feelings and experience, improves the interactivity and interest of urban sculpture space and places and endows users with better spiritual experience [3].

Scholars have done a lot of research on the combination of IoT technology and edge computing, new technology, and urban sculpture space. Du [4] proposed that the development of a city should not only have the urban image with the characteristics of the times but also make full use of historical and cultural resources, retain strong local characteristics and historical context, and form a unique urban personality. Urban sculpture is the best form of expression and the "eye of the city," which shows the spiritual outlook of the city and becomes the business card of a city. A good urban sculpture embodies not only the beauty of form but also the guiding sign of a city's spiritual culture. Urban sculpture is also one of the important elements of urban landscape environment. Qiu et al. [5] proposed that with the development of science and technology, more and more science and technology played an important role in urban construction, and IoT technology, as the current mainstream science and technology, had been developed in various industries. Therefore, through IoT technology, urban sculpture is developed, urban design is planned, more reasonable landscape elements are established for the city, and it plays an important role in urban development. Wang et al. [6] proposed a new model to collect reliable data based on the edge computing of the IoT. The nodes were evaluated from multiple dimensions to obtain accurate trust values. By mapping the trust value of the node to the mobile data collector, the best mobile path with high trust was generated.

Jha et al. [7] proposed a novel simulator Internet of Things simulation-Edge (IoTSim-Edge), which captured the behavior of heterogeneous IoT and edge computing infrastructure, and allowed users to test their infrastructure and framework in a simple and configurable way. IoTsim edge extends CloudSim's capabilities to include different features of edge and IoT devices. The effectiveness of IoTsim edge is described using three test cases. To sum up, the current science and technology have made great progress in the IoT, edge computing, and the combination of the two, and the IoT technology has also played a great role in urban design. However, the concept of urban design based on the combination of the IoT and edge computing has not been developed, so more research is needed to integrate the IoT and edge computing. The development of urban sculpture space and place design is an innovative research, which will also make more contributions to urban development.

First, based on the IoT and edge computing combined with user behavior, this work puts forward the combination of Virtual Reality (VR) and urban sculpture space. Additionally, according to the application requirements of VR technology in urban sculpture space, a VR network system is established based on user interest and Field Of View (FOV). Finally, a VR network system is established based on joint cache cooperation and user interest, which proves the effectiveness of the two algorithms for VR technology. The innovation is to use IoT and edge computing technology to design the application model of VR technology in urban planning, comprehensively analyze its application effect, and innovate the technical methods of urban planning. The proposed algorithm has a good reference for the combination of VR technology and urban sculpture and improves the interactivity and experience of urban sculpture space based on user behavior.

2. Method

2.1. An Overview of Theory of Urban Sculpture Space. Urban sculpture is a sculpture work standing in urban public places. In a city with many tall buildings and vertical and horizontal roads, it can alleviate the congestion, rigidity, and singleness caused by the concentration of buildings and can increase the balance on the open space [8]. According to the theory of urban sculpture space, a certain space is designed according to urban sculpture, and enough sculpture is designed to beautify the city. This design space is called urban sculpture space [9]. There are obvious differences between the current urban sculpture and the traditional sculpture in terms of concept and function. Urban sculpture is mainly aimed at the public and has publicity. The design of sculpture needs to be considered from the following aspects, as shown in Figure 1.

Nowadays, with the development of the IoT, the combination of the IoT and urban sculpture is more in line with modern needs [10]. The combination of digital technology and urban sculpture breaks the form of traditional static sculpture. Through combining them, a variety of urban sculptures appear, and the presented forms are more colorful. The urban sculpture is also more life-like and popular,

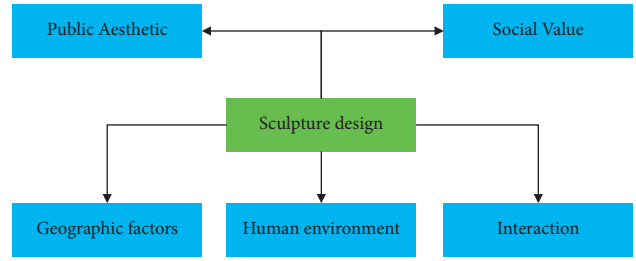

Figure 1: Framework of design considerations for urban sculpture.

and architecture and installation art can be displayed in the form of sculpture; any landscape and landmark also can be presented in the form of sculpture, and all small street sculptures to large architectural landscapes are all modern urban sculptures [11]. The places of urban sculpture space are studied, which focuses on the design of the places. These also emphasize the participation of users, serving users, and classifying them in terms of functions by the behavior of users and the characteristics of the space, as shown in Figure 2.

One of the important attributes of urban sculpture is its spatial attribute. The sculpture is not only a work of art but can also convey the corresponding information of the urban and space to the public. The artistic effect of urban sculpture and the interaction of the spatial environment complement each other. The sculpture not only needs to consider various specific environmental factors of the environment in its design but also needs to coordinate with the spatial environment. The sculpture itself also affects the environment in which it is located and improves the spatial environmental quality of the place [12]. The interactive sculpture in urban sculpture can improve the function of the space, increase the vitality of the space, and enhance the spirit of the space.

2.2. A New Technology of Interactive Urban Sculpture. With the development of IoT and digital technology, the combination of multimedia technology and art came into being, allowing people to participate in sculpture art and get a variety of different feelings. This open art mainly highlights the experience and feeling brought by the work itself, so it is also a challenge to the traditional sculpture art [13]. Traditional sculpture art combines digital technology and IoT technology, changing from static existence to dynamic existence. There are many ways to combine digital technology with urban sculpture. Usually, IoT technology is used to design software, and electronic devices are added to the urban sculpture itself. For example, using 3D modeling, augmented reality (AR) or VR and other IoT technologies, these technologies show the colorful and vibrant urban sculpture art [14]. As one of the main IoT technologies in the art reform, the current three-dimensional digital art has played an important role in urban sculpture. Its fundamental connotation is three-dimensional design, which is the basis of a new generation of digital, virtual, and intelligent design platform. It is a new design method based on plane and two-dimensional design, which makes the design goal more three-dimensional and visual.

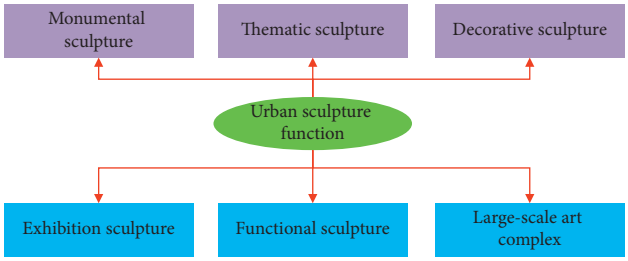

Figure 2: Classification of functions of urban sculpture space.

The traditional urban sculpture is to place the completed sculpture directly on the site and integrate the sculpture and space. Works are less designed from the perspective of user behavior. For users, the feeling given by urban sculpture is a single psychological feeling of looking up [15]. Users are just admirers of urban sculpture. The interaction between users and urban sculpture is poor, and lack interest and the single form of interaction, which cannot make users become real participants [16]. The combination of the IoT technology and urban sculpture greatly improves the interactivity compared with traditional urban sculpture. Urban sculpture using the IoT technology pays more attention to users' feelings and experience, narrowing the distance between users and sculpture art [17]. The combination of the IoT technology and urban sculpture is complementary, and the two cannot be replaced each other. The IoT technology can help urban sculpture better improve its interest and interactivity. Combining the characteristics of urban sculpture with new technologies can better provide users with spiritual experience [18].

2.3. VR Network System Model Based on User Interest and FOV. With the development of the IoT and the upgrading of related equipment, VR technology can be well combined with urban sculpture in urban sculpture spaces. It can create an interesting and interactive space for users [19]. In the urban sculpture space, if VR technology is to bring a good experience to users, the problem is that it needs to meet the requirements of low latency and consume a lot of network resources. These are also the problems that the current VR technology needs to be improved [20]. Mobile edge computing (MEC) can provide good help for the pressure of network resources brought by VR. MEC servers are deployed at the edge of the network, which can improve the computational capability and data caching capability of the network, reduce user latency, and reduce network congestion [21]. Song et al. [22] used mobile edge computing (MEC) to extract FOV videos from 360-degree videos to avoid transmission bandwidth occupation and backhaul link traffic between the base station and the core network. The cache placement and FOV selection of wireless VR service network are studied. Joint content caching and FOV selection are expressed as an optimization problem, which aims to maximize the utility function of the system under the existing network resources. For multivariable-coupled nonconvex problems, a joint optimization algorithm of resource allocation and FOV is proposed, and the algorithm is evaluated by Taylor expansion and successive convex optimization. The results show that the joint optimization algorithm of resource allocation and FOV can effectively meet the delay period and maximize the system revenue under the efficient use of resources. The specific network framework is shown in Figure 3.

In Figure 3, there are M cells, N users in each cell, and H types of videos in the system. According to the visual characteristics of the human eye, the FOV video is transmitted to the users. The viewport size when user n requests h in the M cell is $f_{m,n,h} \in \{\theta_1, \ldots, \theta_k\}$ in which $f_{m,n,h}$ is the viewport angle. When multiple different versions of the same type of FOV video are stored in the MEC, it will take up too much storage space. Therefore, the FOV video is stored in the MEC in a format of 360°, and the optimized strategy is used to process it as a transmission of FOV video [23].

When a user sends a service request to the base station, different revenue settings are performed by the system for videos with different viewport angles. If it is found that the video requested by the user's service is in the cache of the MEC, the MEC can directly send the video from the cache to the user, which can save the transmission bandwidth, and the resulting gain is shown in equations (1)–(3).

$$G_{m,n,h} = \varnothing * \frac{f_{m,n,h}}{360^{\circ}}, \tag{1}$$

$$G_{\text{reward}} = \sum_{m=1}^{M} \sum_{n=1}^{N} \sum_{h=1}^{H} \rho_{m,n,h} G_{m,n,h}, \tag{2}$$

$$G_{\text{cach}} = \alpha \sum_{m=1}^{M} \sum_{n=1}^{N} \sum_{h=1}^{H} \rho_{m,n,h} X_{m,h} r^{\text{mec}}. \tag{3}$$

$G_{m,n,h}$ user n brings benefits to video h in cell m. $\varnothing$ the weight coefficient of return. $\rho_{m,n,h}$ the popularity video. $X_{m,h}$ cache Set. α unity gain of saving bandwidth. r^{mec} transmission rate of sending video content. There is always a cache overhead when caching video in the MEC. Even if the user does not request it, it will occupy the cache space and consume the cache. The 360° video is stored in the system, which needs to be processed by the MEC, and the FOV video requested by the user is extracted from the 360° video and sent to the user. If the cache of the video is not requested in the MEC, and the video is fetched from the core network. There are two processing schemes. One is that the core network performs video processing, and the 360° video is processed as FOV video and sent. The other is that the 360° video is sent first, and then the cell performs video processing and processes it into FOV video. To save transmission resources and reduce latency, the first scheme is adopted. The specific equation is shown in (4)–(7):

$$C_{\text{cach}} = \delta S_{360} \sum_{m=1}^{M} \sum_{h=1}^{H} X_{m,h}, \tag{4}$$

$$C^{1}_{\text{compute}} = \beta \sum_{m=1}^{M} \sum_{n=1}^{N} \sum_{h=1}^{H} \rho_{m,n,h} z^{\text{mec}}_{m,n,h}, \tag{5}$$

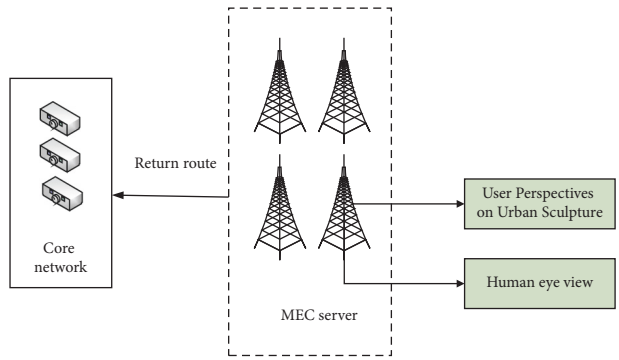

Figure 3: A model of VR network based on user interest and FOV.

$$C^2_{\text{compute}} = \beta \sum_{m=1}^{M}\sum_{n=1}^{N}\sum_{h=1}^{H} \rho_{m,n,h} z^{\text{core}}_{m,n,h}, \tag{6}$$

$$C_{\text{compute}} = \beta \sum_{m=1}^{M}\sum_{n=1}^{N}\sum_{h=1}^{H} \left(\rho_{m,n,h} X_{m,h} z^{\text{mec}}_{m,n,h} + \rho_{m,n,h}\left(1 - X_{m,h}\right) z^{\text{mec}}_{m,n,h}\right), \tag{7}$$

δ is the unity overhead of storage space. S_360 is the size of cache 360°video. $z^{mec}_{m,n,h}$ is the overhead of MEC calculation. β is the unit calculation cost. $z^{core}_{m,n,h}$ is the core network resources of consuming. $z^{core}_{m,n,h} = \eta * f_{m,n,h}/360^\circ$. When the video is transmitted to the user, the video cache is requested by the user in the MEC. The MEC directly provides the user with the content. When the requested video cache is not in the MEC, the content is sent from the core network to the base station, and the base station sends it to the user. The specific equation is shown in (8)–(11):

$$C_1 = \alpha \rho_{m,n,h} r^{\text{user}}_{m,n,h}, \tag{8}$$

$$r^{\text{user}}_{m,n,h} = \sum_{k=1}^{K} B^{\text{user}}_k * \log_2\left(1 + \frac{p_m g_{m,n,k} X_{m,n,k}}{\sum_{m^*=1, m^* \neq m}^{M} \sum_{n=1}^{N} p_m * g_{m^*,n,k} X_{m,n,k} + \sigma^2}\right), \tag{9}$$

$$C_2 = \alpha \rho_{m,n,h} r^{user}_{m,n,h} + \alpha \rho_{m,n,h} r^{mec}, \tag{10}$$

$$C_{\text{transmission}} = \alpha \sum_{m=1}^{M}\sum_{n=1}^{N}\sum_{h=1}^{H} \left(\rho_{m,n,h} z^{\text{user}}_{m,n,h} + \rho_{m,n,h}\left(1 - X_{m,h}\right) r^{\text{mec}}\right). \tag{11}$$

$r^{\text{user}}_{m,n,h}$ is the MEC user transmission rate in the cell. B^{user}_k is the channel bandwidth of user downlink. σ^2 is the additive white Gaussian noise. $X_{m,n,k}$: whether the channel is occupied. If the requested content is not in the MEC, the core network needs to process video, and the processing time is shown in equations (12)–(14):

$$T^{up}_{m,n,h} = A + \left(1 - X_{m,h}\right) B, \tag{12}$$

$$T_3 = \frac{S_{m,n,h}}{R_m}, \tag{13}$$

$$T_4 = \frac{S_{m,n,h}}{R_c}. \tag{14}$$

A is the requested time of uplink. B is the requested time of base station uplink to the core network. $S_{m,n,h}$ is the size of the requested video. $1/R_m$ is the MEC processing time of 1 bit. $1/R_c$ is the core network processing time of 1 bit. According to the above equation, when the user sends the request, the processing time is calculated. The time when the MEC is sent to the user, the time when the core network is sent to the base station, and the time of complete transmission delay are shown in equations (15)–(19):

$$T^{\text{process}}_{m,n,h} = X_{m,h} \frac{S_{m,n,h}}{R_m} + \left(1 - X_{m,h}\right) \frac{S_{m,n,h}}{R_c}, \tag{15}$$

$$T_5 = \frac{S_{m,n,h}}{r^{\text{user}}_{m,n,h}}, \tag{16}$$

$$T_6 = \frac{S_{m,n,h}}{r^{mec}}, \tag{17}$$

$$T^{\text{transmission}}_{m,n,h} = \frac{S_{m,n,h}}{r^{user}_{m,n,h}} + \left(1 - X_{m,h}\right) \frac{S_{m,n,h}}{r^{mec}}, \tag{18}$$

$$T_{m,n,h}^{\text{total}} = T_{m,n,h}^{up} + T_{m,n,h}^{\text{process}} + T_{m,n,h}^{\text{transmission}} = +\left(1 - X_{m,h}\right)B + X_{m,h}\frac{S_{m,n,h}}{R_m} + \frac{S_{m,n,h}}{r_{m,n,h}^{\text{user}}} + \left(1 - X_{m,h}\right)\frac{S_{m,n,h}}{R_c} + \left(1 - X_{m,h}\right)\frac{S_{m,n,h}}{r^{mec}}. \quad (19)$$

By optimizing the cache scheme of MEC and the cell channel allocation of the user's viewport strategy, the situation of optimally allocating resources is shown in equation (20):

$$\begin{aligned}
&\max_{\{f_{m,n,h}\}\{X_{m,h}\}\{X_{m,n,k}\}} U,\\
&s.t.D1:\ A + \left(1 - X_{m,h}\right)B + X_{m,h}\frac{S_{m,n,h}}{R_m} + \frac{S_{m,n,h}}{r_{m,n,h}^{\text{user}}} + \left(1 - X_{m,h}\right)\frac{S_{m,n,h}}{R_c} + \left(1 - X_{m,h}\right) \cdot \frac{S_{m,n,h}}{r^{mec}} \le T_D, \quad \forall m \in M, \quad \forall n \in N,\\
&D2:\ X_{m,h} \in \{0,1\}, \quad \forall m, h,\\
&D3:\ \sum_{h=1}^{H} X_{m,h} S_{360} \le S_m, \quad \forall m \in M,\\
&D4:\ X_{m,n,k} \in \{0,1\}, \quad \forall m, n, k,\\
&D5:\ \sum_{n=1}^{N}\sum_{k=1}^{K} X_{m,n,k} = K, \quad \forall m,\\
&D6:\ \sum_{n=1}^{N} X_{m,n,k} = 1, \quad \forall m, k\\
&D7:\ f_{m,n,h} \in \{\theta_1, \theta_2 \ldots, \theta_k\}, \quad \forall m, n, h.
\end{aligned} \quad (20)$$

In the equation, $D1$ is the user's maximum tolerable delay. $D2$ is the cache constraint. $D3$ is the maximum cache capacity limit of MEC. $D4$ is the channel constraint. $D5$ and $D6$ are the guarantees that the channel is only occupied once, $D7$ is the viewport constraint of FOV. $D2$, $D4$, and $D7$ are integer constraints. $D1$ is a nonconvex constraint, which is a problem of an nonconvex optimization.

2.4. The Solving Algorithm of Problems of VR Network System Model Based on User Interest and FOV. An efficient iterative algorithm is proposed by using variable relaxation, Lagrangian decomposition and other methods. The three subproblems are alternately iterated to obtain the optimal scheme of resource allocation. First, the placement method of the MEC cache is optimized, as shown in equation (21):

$$\begin{aligned}
p1:\ &\max_{\{X_{m,h}\}} \alpha \sum_{m=1}^{M}\sum_{n=1}^{N}\sum_{h=1}^{H} \rho_{m,n,h} X_{m,h} r^{\text{mec}}\\
&- \alpha \sum_{m=1}^{M}\sum_{n=1}^{N}\sum_{h=1}^{H}\left(\rho_{m,n,h}\left(1 - X_{m,h}\right)r^{\text{mec}}\right)\\
&s.t. - \delta S_{360}\sum_{m=1}^{M}\sum_{h=1}^{H} X_{m,h} - \beta \sum_{m=1}^{M}\sum_{n=1}^{N}\sum_{h=1}^{H}\\
&\cdot\left(\rho_{m,n,h} X_{m,h} z_{m,n,h}^{\text{mec}} + \rho_{m,n,h}\left(1 - X_{m,h}\right)z_{m,n,h}^{\text{core}}\right)D1 - D3,
\end{aligned} \quad (21)$$

$p1$ is the problem of standard linear programming. $D7$are the constraints of convex multiple discrete-value. Finally, the method of cell channel allocation is optimized. The use function of system efficiency and the objective function, etc., are shown in equations (22)–(23):

$$U = \alpha \sum_{m=1}^{M}\sum_{n=1}^{N}\sum_{h=1}^{H} \rho_{m,n,h} \sum_{k=1}^{K} B_k^{\text{user}} * \log_2\left(\frac{\sum_{m'=1,m'\neq m}^{m}\sum_{n=1}^{N} p_m \cdot g_{m',n,k} X_{m,n,k} + \sigma^2}{\sum_{m'=1,m'\neq m}^{M}\sum_{n=1}^{N} p_m \cdot g_{m',n,k} X_{m,n,k} + \sigma^2 + p_m g_{m,n,k} X_{m,n,k}}\right), \quad (22)$$

$$\begin{aligned}
U = \alpha \sum_{m=1}^{M}\sum_{n=1}^{N}\sum_{h=1}^{H} \rho_{m,n,h} \sum_{k=1}^{K} B_k^{\text{user}} \Bigg[&\log_2\left(\sum_{m'=1,m'\neq m}^{M}\sum_{n=1}^{N} p_{m'} g_{m',n,k} X_{m,n,k} + \sigma^2\right)\\
&- \log_2\left(\sum_{m'=1,m'\neq m}^{M}\sum_{n=1}^{N} p_m' g_{m',n,k} X_{m,n,k} + \sigma^2 + p_m g_{m,n,k} X_{m,n,k}\right)\Bigg].
\end{aligned} \quad (23)$$

U is the objective function. $X_{m,n,k}$ is the variable. t is number of iterations; $p3$ is the problem of convex programming. The joint placement cache and joint optimization of resource allocation and FOV strategy (J-RAF) are proposed. The computational complexity is $\mathcal{O}(\tau(MH)^2 + (MH) + (MNH))$.

2.5. VR Network System by the Joint Cache Cooperation and User Interest. In the VR wireless network, the panoramic video service has the characteristics of high data, low latency, and many viewing angles [24]. The main research is to use the MEC-assisted VR wireless network to maximize the efficiency of each part of the system, and a resource allocation optimization algorithm is proposed to solve it. In the specific system model, the number of cells is set to M, the number of users in a single cell is set to N, the video category is set to H in the system, and the user viewport is set to $f_{m,n,h}, f_{m,n,h} \in \{\theta_1, \ldots, \theta_k\}$. The specific system model is shown in Figure 4.

The user first sends a request to the base station, and the system is proportional to the income according to the size of the FOV video. The income of the cell and the total income of the system are shown in equations (24)–(27). The cache can save the bandwidth of the backhaul link, and this part of the bandwidth is called caching gain. There is also caching gain in the transmission of user-requested video and adjacent cooperative cells. However, if the video in the cache is not the video requested by the user, these videos will also occupy resources of system, and the total overhead of system is as shown in equations (24)–(27):

$$G_{m,n,h} = \varnothing^* \frac{f_{m,n,h}}{360^\circ}, \tag{24}$$

$$G_{\text{reward}} = \sum_{n=1}^{N} \sum_{h=1}^{H} p_m(h) G_{m,n,h}, \tag{25}$$

$$G_{\text{cach}} = \alpha \sum_{n=1}^{N} \sum_{h=1}^{H} P_m(h) X_{\text{m},h} r^{\text{mec}}, \tag{26}$$

$$G_{\text{cach}} = \delta S_{360} \sum_{m=1}^{N} \sum_{h=1}^{H} X_{\text{m},h}. \tag{27}$$

$\varnothing$ is the gain coefficient, $p_m(h)$ is the distribution of content popularity, α is the unity gain, $X_{\text{m},h}$ is the cache set, r^{mec} is the transmission rate is sent by the core network to the cell. δ is the unit cache overhead, S_{360} is the size of 360° video. The videos of all the users finally receive FOV, and the system needs to process and calculate 360° videos, and the consumption of system resources is proportional to the size of the processed FOV videos. If mmc1 are the adjacent cells that cannot cooperate, or the user requests that the content is not cached, the first method is that the core network can only process the video as FOV video, or the core network directly sends the video to the cell for processing by the cell itself. The second method can save some transmission bandwidth and reduce latency. The processed content is transmitted to the user, and there are two transmission overheads corresponding to the two scenarios, and there are a cache of requested videos in the MEC and no requested video in the MEC of the cell where it is located. However, there is a cache in the adjacent cooperative cells, and the adjacent cells can transfer cooperatively. The specific transmission overhead is shown in equation (28):

$$\begin{aligned}
C_1 &= \alpha P_{m,h} r^{\text{user}}_{m,n,h} \\
C_2 &= \alpha P_{m,h} r^{\text{user}}_{m,n,h} + \alpha P_m(h) \\
&\quad \cdot \left(1 - X_{m,h}\right) \sum_{m^* \neq m} X_{m^*,h} Y(h) r^{\text{cell}} \\
C_3 &= \alpha P_{m,h} r^{\text{user}}_{m,n,h} + \alpha P_m(h) \\
&\quad \cdot \left(1 - X_{m,h}\right) \left(1 - \sum_{m^* \neq m} X_{m^*,h}\right) r^{\text{core}} \\
&\quad + \alpha P_m(h) \left(1 - X_{m,h}\right) \\
&\quad \cdot \sum_{m^* \neq m} X_{m^*,h} (1 - Y(h)) r^{\text{core}} \\
C_{\text{transmission}} &= \sum_{N} \sum_{H} \alpha P_m(h) r^{\text{user}} + \sum_{N} \sum_{H} \alpha P_m(h) \\
&\quad \cdot \left(1 - X_{m,h}\right) \sum_{m^* \neq m} X_{m^*,h} Y(h) r^{\text{cell}} \\
&\quad + \sum_{N} \sum_{H} \alpha P_m(h) \left(1 - X_{m,h}\right) \\
&\quad \cdot \sum_{m^* \neq m} X_{m^*} (1 - Y(h)) r^{\text{core}} \\
&\quad + \sum_{N} \sum_{H} \alpha P_m(h) \left(1 - X_{m,h}\right) (1 - Y(h)) r^{\text{core}}.
\end{aligned} \tag{28}$$

β is unit processing cost. $z^{mec}_{m,n,h}$ is MEC computing processing overhead. $z^{core}_{m,n,h}$ is the computing processing overhead of the core network. $r^{\text{user}}_{m,n,h}$ is the transmission rate of user. r^{cell} is the cell transmission rate. r^{core} is the transmission rate from core network to cell. When users use VR, the network needs to meet the requirements of low latency, and it is necessary to calculate the delay of each link. When the content requested by the user is not in the MEC, the video is processed through the core network. The processing delay and the transmission delay from the MEC to the user are shown in equation (29):

$$\begin{aligned}
T_4 &= \frac{S_{m,n,h}}{R_c} T^{\text{process}}_{m,n,h} \\
&= X_{m,h} \frac{S_{m,n,h}}{R_m} + \left(1 - X_{m,h}\right) \frac{S_{m,n,h}}{R_m} \sum_{m^* \neq m} X_{m^*,h} Y(h) \\
&\quad + \left(1 - X_{m,h}\right) \frac{S_{m,n,h}}{R_c} \sum_{m^* \neq m} X_{m^*,h} (1 - Y(h)) \\
&\quad + \left(1 - X_{m,h}\right) \frac{S_{m,n,h}}{R_c} \left(1 - \sum_{m^* \neq m} X_{m^*,h}\right) T_5 \\
&= \frac{S_{m,n,h}}{r^{\text{user}}_{m,n,h}}.
\end{aligned} \tag{29}$$

$S_{m,n,h}$ is the size of the requested video. $1/R_m$ is MEC processing time of 1 bit。 $1/R_c$ is the core network processing time of 1 bit. $T^{process}_{m,n,h}$ is the processing delay of service calculation. If the content is in adjacent cells, the cells can transfer

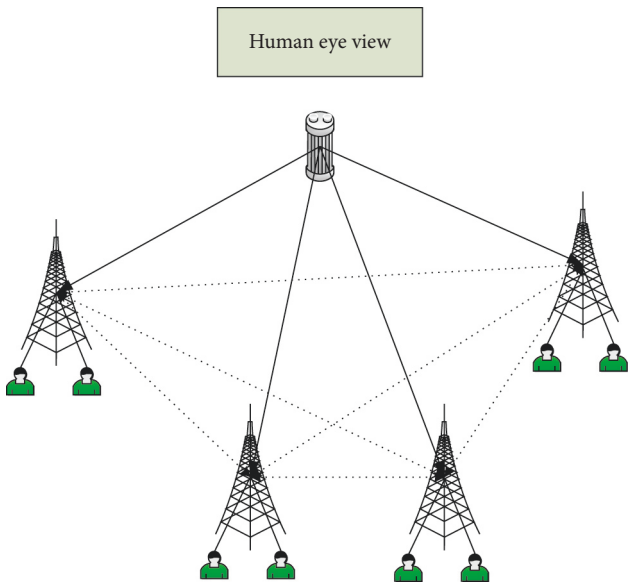

Figure 4: The diagram of VR Network System by the joint cache cooperation and user interest.

cooperatively. If the adjacent cells cannot transfer cooperatively, they need to be transmitted from the core network. The two transmission delays are shown in equation (30):

$$\begin{aligned} T_6 &= \frac{S_{m,n,h}}{r^{\text{cell}}} + T_{\text{queue}} T_7 \\ &= \frac{S_{m,n,h}}{r^{\text{core}}} T^{\text{process}}_{m,n,h} \\ &= \frac{S_{m,n,h}}{r^{\text{user}}_{m,n,h}} + \left(1 - X_{m,h}\right)\left(1 - \sum_{m^* \neq m} X_{m^*,h}\right)\frac{S_{m,n,h}}{r^{\text{core}}} \\ &\quad + \left(1 - X_{m,h}\right)\left(\frac{S_{m,n,h}}{r^{\text{cell}}} + T_{\text{queue}}\right)\sum_{m^* \neq m} X_{m^*,h} Y \\ &\quad + \left(1 - X_{m,h}\right)\frac{S_{m,n,h}}{r^{\text{core}}}\sum_{m^* \neq m} X_{m^*,h}(1 - Y) T^{\text{total}}_{m,n,h} \\ &= T^{\text{up}}_{m,n,h} + T^{\text{process}}_{m,n,h} + T^{\text{transmission}}_{m,n,h}. \end{aligned} \tag{30}$$

The system utility function of the VR network system and of joint cache cooperation and user interest is shown in equation (31) and the problem of optimization is shown in equation (32). $\{X_{m,h}\}$ is MEC cache placement, $\{f_{m,n,k}\}$ is the viewport allocation of user. $\{Y_h\}$is the strategy of cooperative cache.

$$U = G_{\text{reward}} + G_{\text{cach}} - C_{\text{cach}} - C_{\text{transmission}} - C_{\text{compute}}, \tag{31}$$

$$\begin{aligned} &\max_{\{f_{m,n,h}\}\{X_{m,h}\}\{X_{m,n,k}\}} U \\ &D1\colon T^{\text{total}}_{m,n,h} \le T_D, \quad \forall m \in M, \quad \forall n \in N, \\ &D2\colon X_{m,h} \in \{0,1\}, \quad \forall m, h, \\ &D3\colon \sum_{h=1}^{H} X_{m,h} S_{360} \le S_m, \quad \forall m \in M, \\ &D4\colon Y_h \in \{0,1\}, \quad \forall h, \\ &D5\colon f_{m,n,h} \in \{\theta_1, \theta_2 \ldots, \theta_k\}, \quad \forall m, n, h, \\ &D6\colon \sum_{m^* \neq m} X_{m^*,h} \in \{0,1\}. \end{aligned} \tag{32}$$

$D1$ is the maximum delay of gratification of the user, which needs to ensure a good experience for users. $D2$ is the strategy of MEC cache prevention. $D3$ is the limit of MEC maximum cache capacity. $D4$ is the cooperative transmission strategy of adjacent cells. $D6$ is to select one of the cells of caching multiple requested content for cooperative transmission. $D1$ is a nonconvex constraint, which is a problem of nonconvex optimization.

2.6. The Solving Algorithm of Problems of VR Network System Based on Joint Cache Cooperation and User Interest. The problem of nonconvex optimization is divided into three methods to solve. The first method is the optimization of the MEC cache placement, as shown in equation (33). Through the transformation and deformation, the equation (34) can be obtained. Finally, the optimization method of the cache is obtained by solving, as the input of the next question.

$$\begin{aligned} p2\colon &\max_{\{X_{m,h}\}} \alpha \sum_{n=1}^{N}\sum_{h=1}^{H} P_m(h) X_{m,h} r^{\text{mec}} - \delta S_{360} \sum_{h=1}^{H} X_{m,h} \\ &- \left[\begin{array}{l} \beta \sum_{n=1}^{N}\sum_{h=1}^{H} P_m(h) z^{\text{mec}}_{m,n,h} + \beta \sum_{n=1}^{N}\sum_{h=1}^{H} P_m(h)\left(1 - X_{m,h}\right) z^{\text{mec}}_{m,n,h} \sum_{m^* \neq m} X_{m^*,h} Y(h) + \beta \sum_{n=1}^{N}\sum_{h=1}^{H} P_m(h)\left(1 - X_{m,h}\right) z^{\text{core}}_{m,n,h} \sum_{m^* \neq m} X_{m^*,h} Y(h)\left(1 - \sum_{m^* \neq m} X_{m^*,h} Y(h)\right) \\ \quad + \alpha \sum_{n=1}^{N}\sum_{h=1}^{H} P_m(h)\left(1 - X_{m,h}\right) \sum_{m^* \neq m} X_{m^*,h} Y(h) r^{\text{cell}} + \sum_{n=1}^{N}\sum_{h=1}^{H} P_m(h)\left(1 - X_{m,h}\right)\left(1 - \sum_{m^* \neq m} X_{m^*,h} Y(h)\right) r^{\text{core}} \end{array}\right] \end{aligned} \tag{33}$$

$$f_1(x)f_2(x) = \frac{\left(f_1(x)+f_2(x)\right)^2}{2} - \frac{f_1(x)^2+f_2(x)^2}{2} \left(f_1(x)+f_2(x)\right)^2 \geq \left(f_1^r(x)+f_2^r(x)\right)^2 + 2\left(f_1^r(x)+f_2^r(x)\right)\left(f_1(x)-f_1^r(x)\right) + 2\left(f_1^r(x)+f_2^r(x)\right)\left(f_2(x)-f_2^r(x)\right). \tag{34}$$

The second is to fix the MEC cache settings and cooperative transfer method to transform the original optimization problem $p2$ into a tractable problem $p3$, as shown in equation (35). D5 is the convex multidiscrete value constraint. The third is to give the cache settings viewport allocation method of users, which can convert $p3$ to $p4$, as shown in equation (36):

$$\begin{aligned} &\max Q(t)W_{\text{coo}} \sum_{h=1}^{H}\sum_{m}^{M} p_m(h)\left(1-X_{m,h}\right)S_{360}f_{m,h}Y_{m,h}\sum_{m^*\neq m}X_{m^*,h} \\ &+ Q(t)W_{\text{bh}} \sum_{h=1}^{H}\sum_{m=1}^{M} p_m(h)S_{360}f_{m,h}\left(1-X_{m,h}\right)\left(1-Y_{m,h}\sum_{m^?\neq m}X_{m^*,h}\right) s.t.D4, \end{aligned} \tag{35}$$

$$\begin{aligned} &\min Q(t)W_{\text{coo}} \sum_{h=1}^{H}\sum_{m}^{M} p_m(h)\left(1-X_{m,h}\right)S_{360}f_{m,h}Y_{m,h}\sum_{m^*\neq m}X_{m^*,h} \\ &- Q(t)W_{\text{bh}} \sum_{h=1}^{H}\sum_{m=1}^{M} p_m(h)S_{360}f_{m,h}Y_{m,h}\sum_{m^*\neq m}X_{m^*,h} s.t.D3. \end{aligned} \tag{36}$$

$D3$ is binary variable constraints. According to the above three methods, the MEC cache setting, FOV allocation of user, and cooperative caching strategy are optimized and solved. The Binary Code Decimal (BCD) algorithm is used to propose an algorithm of resource allocation, Joint Cooperative Content Caching and FOV (J-CCF), that combines MEC cache setting, FOV allocation of user, and cooperative transmission optimization. Cooperative Content Caching and FOV, J-CCF, and the computational complexity of J-CCF algorithm are $\mathcal{O}(\tau(MH)^2 + (MH) + (MH))$.

3. Result

3.1. An Analysis of Experimental Results of VR Network System Using User Interest and FOV. The relationship between the VR network system of user interest and FOV and the number of iterations, and between the efficiency function and the number of users are shown in Figure 5.

Figure 5(a) shows the relationship between the system efficiency of the VR network and FOV and the number of iterations. It is obvious that the J-RAF algorithm has the best performance among the three comparisons between the J-RAF algorithm, the random cache strategy, and the random viewport strategy. Moreover, the J-RAF algorithm becomes convergent after the seventh time, the speed of convergence is fast, and the performance is good. The proposed J-RAF algorithm also has the best performance. Figure 5(b) indicates the relationship between system return and the number of users. As the number of users increases, the efficiency function of the system also increases gradually, and the increase becomes more and more gentle. The relationship between system benefit and the cache space, and between the different cache spaces and user delay times of user are shown in Figure 6.

Figure 6(a) shows the relationship between the size of the cache space and the system benefit. Comparing the J-RAF algorithm, the random cache strategy and the random viewport strategy, the three methods are different. Compared with the other two schemes, the J-CCF algorithm has different performance; the gains are 3% and 20% respectively. However, when the cache space continues to increase, the benefit growth of the system gradually slows down. In Figure 6(b), it is found that the user delay time of the J-RAF scheme and the random viewport scheme increases with the increase of the cache space, mainly because the increase of the cache space can provide users with more services and resources, resulting increase in the delay time. The user delay time of the random caching scheme decreases as the cache space increases, and the delay time decreases because the video does not need to be sent from the core network.

3.2. A Comparative Analysis of VR Network System Results Based on Joint Cache Collaboration and User Interest. The efficiency of the network system varies according to the number of iterations, and the comparative relationship between the efficiency function and the number of users is shown in Figure 7.

Figure 7(a) expresses the relationship between the efficiency of the VR network system and the number of iterations of joint cache cooperation and user interest. It means that the J-CCF algorithm has the best performance among the three comparisons between the cache strategy without cooperation and the random viewport strategy. Moreover, the J-CCF algorithm becomes convergent after the sixth time, the convergence speed is fast, and the convergence performance is good. The proposed J-CCF algorithm has the best performance. Figure 7(b) is a graph showing the

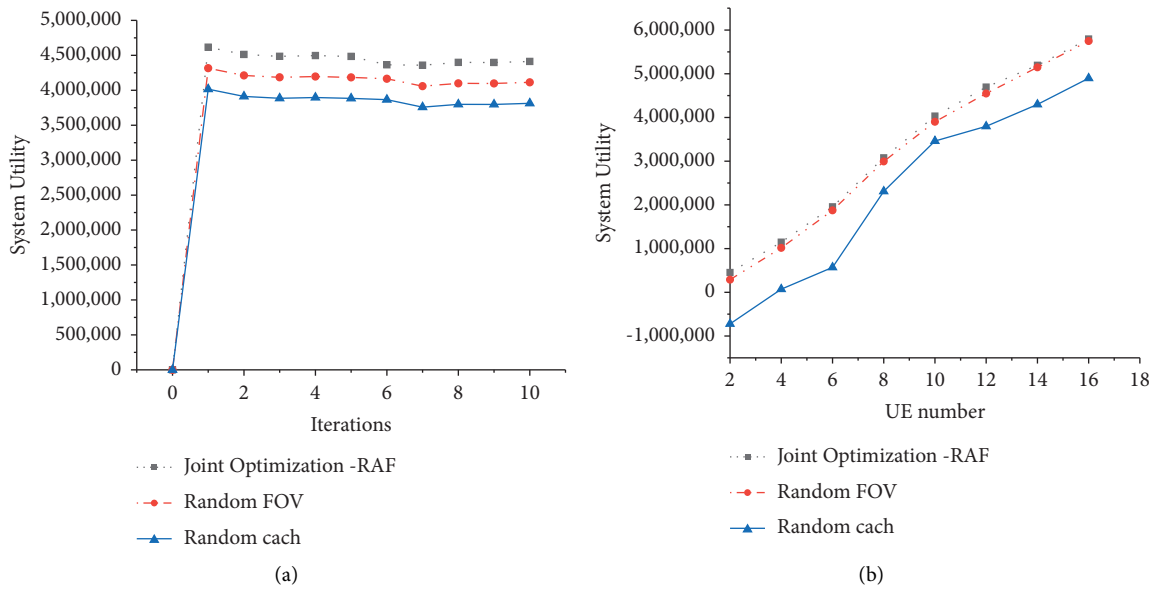

Figure 5: The relationship between the number of users and the system efficiency function according to different optimization schemes: (a) The system efficiency function of different optimization schemes, (b) The system efficiency function of different numbers of users.

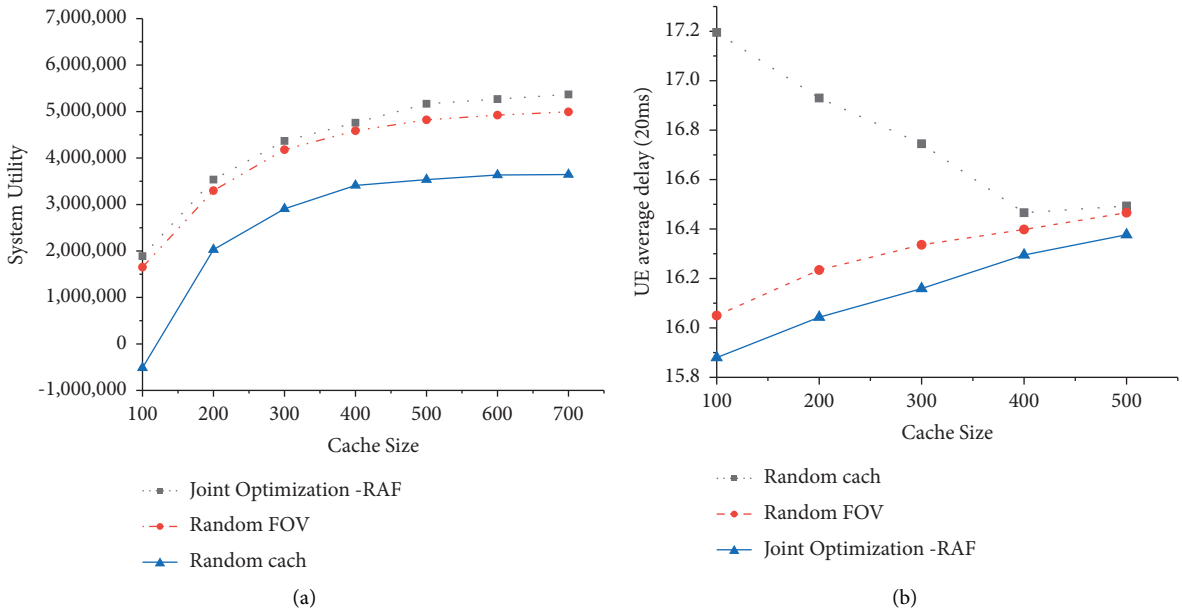

Figure 6: The comparison of the size of caching space, the efficiency function of the system, and the delay time: (a) The efficiency function of the system for different cache spaces, (b) The delay time of user under different cache sizes.

relationship between the system benefit and the number of users. As the number of users increases, the efficiency function of the system also increases gradually, and the increase becomes more and more gentle. And when the number of users is more, it will slowly reach the highest performance of the system. Figure 8 shows the relationship between system benefit and cache space, and the change in cache space and user delay time.

Figure 8(a) represents the relationship between the size of the cache space and the system benefit. Through comparing the J-CCF algorithm, the cache strategy without cooperation, and the random viewport strategy, the J-CCF algorithm has different boosts in terms of performance compared with the other two schemes. The gains are 15% and 25% respectively. However, when the cache space continues to increase, the benefit growth rate of the system gradually slows down. In Figure 8(b), it shows that with the increase of cache space, the average delay time of users increases, and the increase of cache space will provide more services, and the delay time of user will increase slightly. The service rate with and without the strategy is shown in Figure 9.

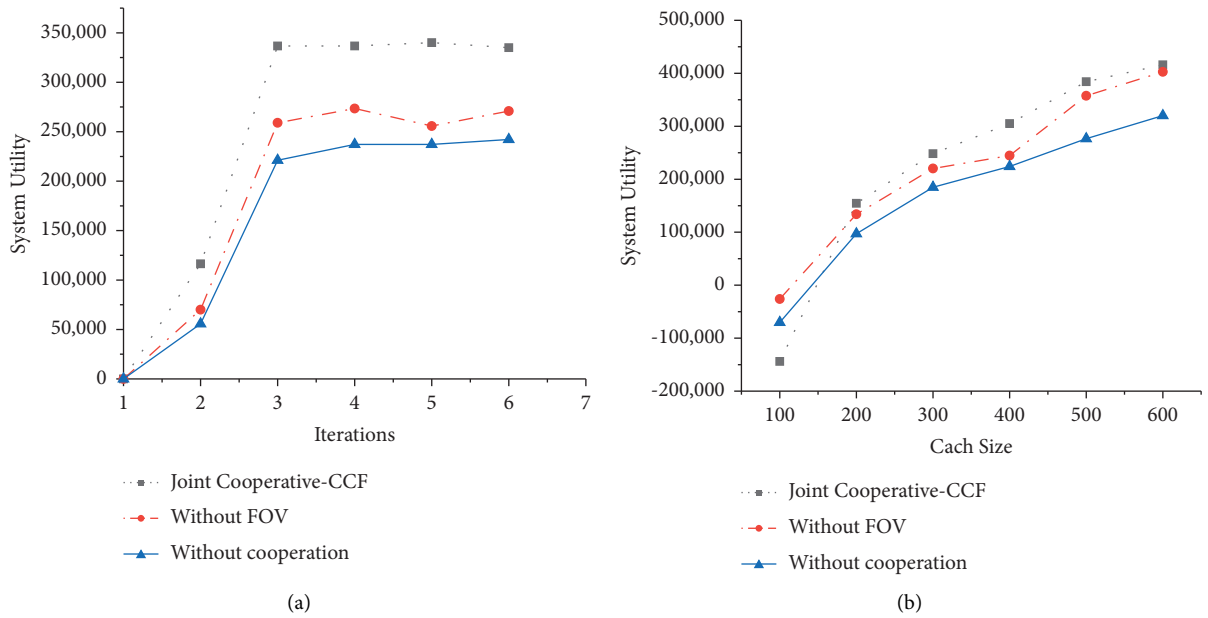

FIGURE 7: The comparison of the performance of J-CFF algorithm and the average system efficiency function under different numbers of users: (a) The performance of J-CFF algorithm, (b) The result of the average system efficiency function for different numbers of users.

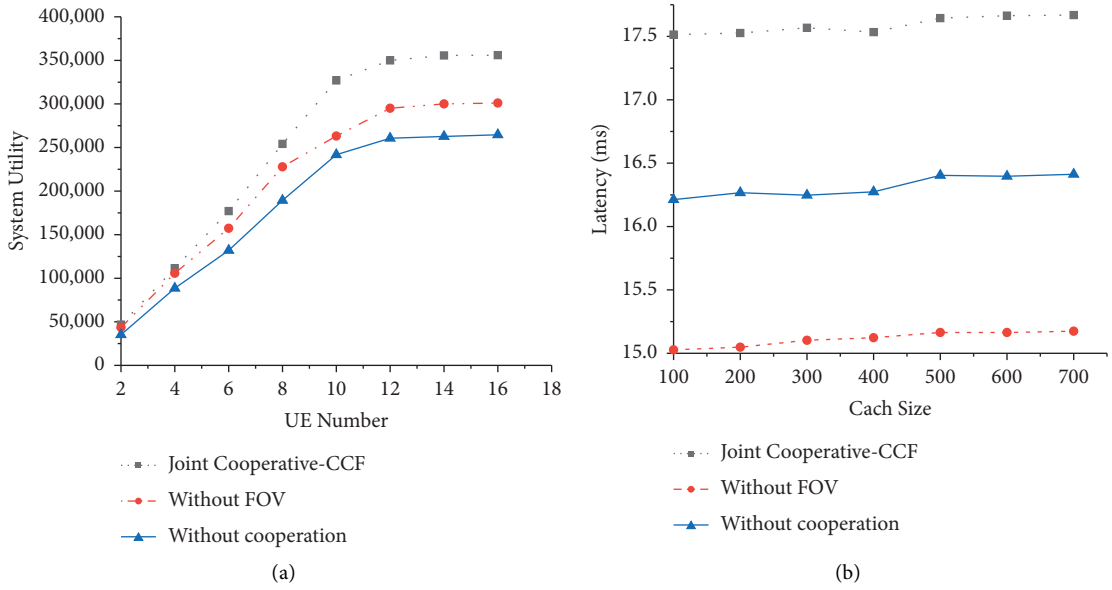

FIGURE 8: The comparison of the size of caching space, the efficiency function of the system, and the delay time: (a) The efficiency function of the system for different cache spaces, (b) The delay time of user under different cache sizes.

Figure 9 indicates that when the cooperation scheme of J-CCF algorithm is adopted, the overall load situation of the service area is more stable and balanced than that of the service area that does not use the J-CCF algorithm. The load situation can be doubled. The variances of the two schemes are 0.00236 and 0.00076, respectively. Using the cooperation scheme of J-CCF algorithm can balance the load and avoid the situation of business concentration, which verifies the effectiveness of the cooperation scheme of J-CCF algorithm.

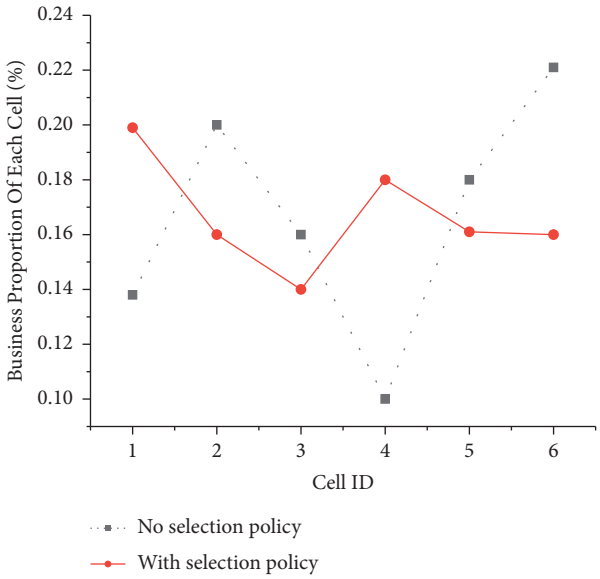

Figure 9: The service rate of each cell before and after the adoption of the scheme.

4. Conclusion

Based on the IoT and edge computing technology, this work analyzes the existing problems of urban sculpture, introduces VR technology into the design of urban sculpture space, and improves the interactivity and experience of urban sculpture space. First, aiming at the introduction of VR technology, to meet the large amount of data and low delay of the IoT required by VR technology, a resource allocation algorithm J-RAF is proposed based on the resource allocation problem of user interest and FOV,, and the effectiveness of J-RAF algorithm is verified by simulation experiments. Second, a VR network system is established based on cache cooperation and user interest, and a resource allocation algorithm J-CCF is proposed. Simulation experiments are used to verify the effectiveness of J-CCF algorithm. Experiments show that J-RAF algorithm can converge faster and has better convergence performance, and has 3% and 20% system gain, respectively. Compared with no cooperative cache scheme and random viewport strategy, J-CCF algorithm can achieve convergence after six iterations, with better convergence performance and 15% and 25% gain in system efficiency. It is proved that the two algorithms are effective for VR technology. The proposed algorithm has a good reference for combining new technology and urban sculpture and improves the interactivity and experience of urban sculpture space based on user behavior. In this work, the use of VR and the setting of user preferences are fixed values, so there is no algorithm in the analysis of user interest and consequently a lack of dynamic calculation of user interest in the calculation process. Hence, the research on resource allocation will be carried out in the future research to strengthen the contribution of dynamic calculation of user interest to the design of urban sculpture space.

Data Availability

The raw data supporting the conclusions of this article will be made available by the authors, without undue reservation.

Ethical Approval

This article does not contain any studies with human participants or animals performed by any of the authors.

Consent

Informed consent was obtained from all individual participants included in the study.

Conflicts of Interest

All authors declare that they have no conflicts of interest.

Authors' Contributions

All authors listed have made a substantial, direct, and intellectual contribution to the work and approved it for publication.

Acknowledgments

The authors acknowledge the help from the university colleagues.

References

[1] F. Yin, H. J. Wen, and X. H. Guo, "Thematic planning of urban sculpture systems: a case study of red sculpture system planning in yan'an," *Journal of Landscape Research*, vol. 12, no. 5, pp. 97–102, 2020.

[2] B. Bachler, "Slowness, streams, and networks in the more-than-human world: prototyping an Internet of things for water," *Journal of Science and Technology of the Arts*, vol. 12, no. 3, pp. 25–44, 2020.

[3] T. Jiang, "Urban public art and interaction design strategy based on digital technology," *Cluster Computing*, vol. 22, no. S2, pp. 3471–3478, 2019.

[4] J. Du, "Research on landscape sculpture design of modern zen and tea theme block," *OALib*, vol. 07, no. 07, pp. 1–8, 2020.

[5] T. Qiu, J. Chi, X. Zhou, Z. Ning, M. Atiquzzaman, and D. O Wu, "Edge computing in industrial Internet of things: architecture, advances and challenges," *IEEE Communications Surveys & Tutorials*, vol. 22, no. 4, pp. 2462–2488, 2020.

[6] T. Wang, L. Qiu, A. K. Sangaiah, A. Liu, M. Z. A. Bhuiyan, and Y Ma, "Edge-computing-based trustworthy data collection model in the Internet of things," *IEEE Internet of Things Journal*, vol. 7, no. 5, pp. 4218–4227, 2020.

[7] D. N. Jha, K. Alwasel, A. Alshoshan et al., "IoTSim-Edge: a simulation framework for modeling the behavior of Internet of Things and edge computing environments," *Software: Practice and Experience*, vol. 50, no. 6, pp. 844–867, 2020.

[8] A. Hochman, "RACSO art gallery presents " "ContraFuerte": conceiving an urban sculpture"," *Sculpture Review*, vol. 68, no. 1, pp. 26–31, 2019.

[9] E. Naseri and A. Nadalian, "The emergence of the horseman sculpture in tehran's urban arts," *Journal of History Culture and Art Research*, vol. 8, no. 2, p. 225, 2019.

[10] W. Cudny and H. Appelblad, "Monuments and their functions in urban public space," *Norsk Geografisk Tidsskrift - Norwegian Journal of Geography*, vol. 73, no. 5, pp. 273–289, 2019.

[11] W. Kuang and Y. Dou, "Investigating the patterns and dynamics of urban green space in China's 70 major cities using satellite remote sensing," *Remote Sensing*, vol. 12, no. 12, p. 1929, 2020.

[12] Y. Chen, J. Zhang, Q. Chen et al., "Three-dimensional printing technology for localised thoracoscopic segmental resection for lung cancer: a quasi-randomised clinical trial," *World Journal of Surgical Oncology*, vol. 18, no. 1, p. 223, 2020.

[13] N. A. A. Gonzalez, F. S. Warden, H. N. Q. Milian, and S. Hosseini, "Interactive design and architecture by using virtual reality, augmented reality and 3D printing," *International Journal of Simulation and Process Modelling*, vol. 15, no. 6, p. 535, 2020.

[14] O. Jean-Baptiste, "Augmented and virtual reality art: a new Frontier of legal protection," *Interactive Entertainment Law Review*, vol. 4, no. 2, pp. 102–111, 2021.

[15] A. Akande, "Manifestations of orí (head) in traditional yorùbá architecture," *IAFOR Journal of Cultural Studies*, vol. 5, no. 2, pp. 5–19, 2020.

[16] C. You and J. Li, "Application of landscape sculpture in interior design-taking wood carving as an example," *OALib*, vol. 07, no. 08, pp. 1–5, 2020.

[17] A. Gor, "Reimagining the iconic in new media art: mobile digital screens and chôra as interactive space," *Theory, Culture & Society*, vol. 36, no. 7-8, pp. 109–133, 2019.

[18] M. Li, T.-C. Hsiao, and C.-C. Chen, "Exploring the factors of cooperation between artists and technologists in creating new media art works: based on AHP," *Sustainability*, vol. 12, no. 19, p. 8049, 2020.

[19] X. I. A. Fan and M. Lü, "New space for city communication: a study on culture transmission by nanjing metro[J]," *Cross-Cultural Communication*, vol. 17, no. 1, pp. 30–34, 2021.

[20] H. Zhao, Q. H. Zhao, and B. Ślusarczyk, "Sustainability and digitalization of corporate management based on augmented/virtual reality tools usage: China and other world IT companies' experience," *Sustainability*, vol. 11, no. 17, p. 4717, 2019.

[21] Y. Wu, J. Pan, Y. Lu, J. Chao, H. Yu, and S. Wan, "Psychotherapy for advanced cancer patients: a meta-analysis of the quality of life and survival assessments," *Palliative & Supportive Care*, vol. 14, pp. 1–7, 2022.

[22] W. Song, Y. Wang, M. Liu, and Z. Fei, "Joint optimization of resource allocation and FOV for VR services in mobile edge networks," in *Proceedings of the 2020 IEEE 6th International Conference on Computer and Communications (ICCC)*, pp. 535–541, Chengdu, China, December 2020.

[23] C. Chen, J. Jiang, Y. Zhou, N. Lv, X. Liang, and S. Wan, "An edge intelligence empowered flooding process prediction using Internet of things in smart city," *Journal of Parallel and Distributed Computing*, vol. 165, no. 3, pp. 66–78, 2022.

[24] I. J. Akpan, D. Soopramanien, and D. H. A. Kwak, "Cutting-edge technologies for small business and innovation in the era of COVID-19 global health pandemic," *Journal of Small Business and Entrepreneurship*, vol. 33, no. 6, pp. 607–617, 2021.